

Rapid bistable reactions in porous catalysts

V.P. Zhdanov^{a,b,*} and B. Kasemo^a

^a Department of Applied Physics, Chalmers University of Technology, S-412 96 Göteborg, Sweden

E-mail: zhdanov@fy.chalmers.se

^b Boreskov Institute of Catalysis, Russian Academy of Sciences, Novosibirsk 630090, Russia

E-mail: zhdanov@catalysis.nsk.su

Received 15 September 2000; accepted 5 December 2000

We analyze the kinetics of rapid bistable reactions (e.g., CO or hydrogen oxidation on Pt) occurring on a nm catalyst particle located inside a mesoscopic pore. Limitations for reactant diffusion inside a single pore are shown to modify the dependence of the reaction rate on the reactant pressures outside the pore. In particular, the position of the maximum reaction rate is shifted to higher CO pressures (provided that the O₂ pressure is fixed). This effect is significant if a pore is not too short. Similar effects are possible during oscillations in CO oxidation on supported nm catalyst particles.

KEY WORDS: nanometer catalysts; support; pores; Knudsen diffusion; diffusion limitations

A major class of real catalysts – so-called supported catalysts – consists of small metal particles deposited on the internal surface of a more or less inactive porous support. In practice, such catalysts are shaped either as porous pellets (2–20 mm in diameter) or monoliths with a porous “wash-coat”. The size of pores varies over a large range from 1–2 (micropores) to ≥ 50 nm (macropores). Often the pores are mesoscopic (2–50 nm). The size of metal particles, d , may vary over a wide range as well (often $d \approx 1$ –20 nm). The reaction kinetics in such catalysts are kinetically controlled if the reaction is slow, while the rate of rapid reactions is limited by reactant diffusion via pores. Quantitatively, the role of diffusion is usually scrutinized by employing the phenomenological reaction–diffusion equations [1]. For example, in the case of the simplest first-order reaction, one has

$$\partial n / \partial t = D_{\text{ef}} \Delta n - k_{\text{ef}} n, \quad (1)$$

where n is the reactant concentration, D_{ef} the effective diffusion coefficient, and $k_{\text{ef}} = k_0 N_c$ the effective reaction rate constant (k_0 is the rate constant corresponding to a single catalyst particle, and N_c is the concentration of catalyst particles). The effectiveness factor, η , is defined as the ratio of the average reaction rate to the rate calculated in the limit when the diffusion limitations are negligible. For a spherical pellet of the radius R , the solution to equation (1) is well known to yield

$$\eta = \frac{3}{\phi} \left[\frac{\cosh \phi}{\sinh \phi} - \frac{1}{\phi} \right], \quad (2)$$

where $\phi = (k_{\text{ef}} R^2 / D_{\text{ef}})^{1/2}$ is the Thiele modulus. For rapid and slow diffusion ($\phi \ll 1$ and $\phi \gg 1$), expression (2) results in $\eta \approx 1$ and $\eta \approx 3/\phi$, respectively.

* To whom correspondence should be addressed.

The conventional mean-field approach outlined above is based on the assumption that the rate constant k_{ef} (or k_0) characterizes the true reaction kinetics. In other words, this constant is usually assumed to be independent of the rate of diffusion, i.e., the interplay of reaction and diffusion inside single pores is not treated explicitly. More recent simulations [2,3] of reaction kinetics in porous solids have analyzed the latter aspect of the problem in detail. Specifically, the first-order reaction was assumed to occur on the catalytically active walls of pores (the results obtained [2] justify application of the phenomenological approach). For supported catalysts, this model makes sense if the pores are so large that there is a multitude of catalytic particles inside a single pore. In mesoscopic pores, this is often not the case. If, for example, the size of catalyst particles is comparable with the pore radius, a single pore will as a rule contain no or only one catalytic particle. Under such circumstances, the reaction rate on a single catalyst particle can be limited by diffusion inside the pore where this particle is located.

The goal of this Letter is to show that the latter regime may occur in such *rapid bistable* reactions as CO or H₂ oxidation on Pt (for a general review of the kinetics of these reactions, see [4]). Specifically, we explicitly illustrate the effect on the bistability diagram of diffusion limitations inside a single pore.

For example, we treat CO oxidation on a Pt, Pd or Rh particle (with linear dimension $d \approx 10$ nm) located at depth l inside a mesoscopic cylindrical pore of length L (figure 1). Adjacent pores (on both sides) are assumed to be free of catalyst particles. The interconnection between pores is considered to be good, i.e., each pore contacts several other pores. In this case, the reactant concentrations near the entrances of the pore under consideration are (nearly) equal to the average concentrations in the pore space outside the pore. If the reaction is rapid, the reactant concentrations near the catalyst

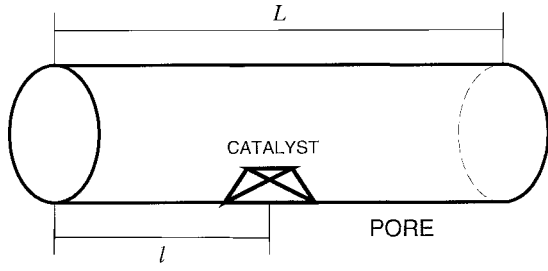
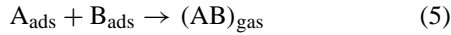


Figure 1. Cylindrical pore containing a catalyst particle. L is the pore length. l is the distance between a catalyst particle and the left-hand-side pore throat.

particle may be appreciably lower than that outside the pore. To calculate the reaction rate in this case, we need to solve the coupled equations describing the reaction kinetics on the catalyst particle and the reactant transport via the pore.

We consider here CO oxidation on Pt, Pd or Rh which is known to occur via the Langmuir–Hinshelwood (LH) mechanism,



where A and B_2 stand for CO and O_2 , respectively.

On nm catalyst particles, the CO oxidation process can be complicated by various factors inherent to the nm-scale chemistry [5] (e.g., by the interplay of reactions on different facets due to reactant diffusion via the interfacet boundaries, etc.). In our present treatment, focused on the role of the reactant transport in pores, such factors are, however, not of central importance. For this reason, we use the simplest mean-field equations in order to describe the reaction kinetics on the catalyst,

$$d\theta_A/dt = k_A^a n_A^l (1 - \theta_A - \theta_B) - k_A^d \theta_A - k_r \theta_A \theta_B, \quad (6)$$

$$d\theta_B/dt = k_{B_2}^a n_{B_2}^l (1 - \theta_A - \theta_B)^2 - k_r \theta_A \theta_B, \quad (7)$$

where θ_A and θ_B are adsorbate coverages, n_A^l and $n_{B_2}^l$ the local reactant concentrations near the catalyst (the superscript l indicates the location of the catalyst (figure 1)), and k_A^a , k_A^d , $k_{B_2}^a$ and k_r the rate constants for adsorption, desorption, and reaction.

To illustrate explicitly the type of kinetics predicted by equations (6) and (7), we assume that the LH step is rapid, i.e., $k_r \rightarrow \infty$. In this limit, the surface is (near the steady state) covered predominantly by either A or B species. When $n_A^l/n_{B_2}^l$ is small, the B_2 adsorption dominates (i.e., $\theta_B \gg \theta_A$ and $\theta \approx \theta_B$, where $\theta = \theta_A + \theta_B$), the A coverage is low, and the A desorption rate is to a first approximation negligible due to rapid reaction of A with B, i.e., the adsorption rate of A is balanced by the AB formation reaction, $k_A^a n_A^l (1 - \theta) \approx k_r \theta_A \theta_B$. Substituting the latter relationship into equation (7), we have

$$d\theta/dt = k_{B_2}^a n_{B_2}^l (1 - \theta)^2 - k_A^a n_A^l (1 - \theta). \quad (8)$$

In analogy, the A dominated regime (where $n_A^l/n_{B_2}^l$ is sufficiently large and $\theta \approx \theta_A$) is described as

$$d\theta/dt = k_A^a n_A^l (1 - \theta) - k_A^d \theta - k_{B_2}^a n_{B_2}^l (1 - \theta)^2. \quad (9)$$

Under the steady-state conditions, equations (8) and (9) correspond, respectively, to the two stable states of the bistable kinetics. To use these equations, we should solve the diffusion equations in order to interconnect the local reactant concentrations, n_A^l and $n_{B_2}^l$, with the concentrations outside the pore, n_A and n_{B_2} . In our simulations, the sticking coefficient of A is for simplicity assumed to be much larger than that of B_2 (this is the case, e.g., for CO and O_2 adsorption on Pt(111)). With this ratio of the sticking coefficients, the gradients in the B_2 concentration are nearly negligible provided that the coefficient of B_2 diffusion is about the same or higher than that for A diffusion (this is the case for CO oxidation). Thus, we need to analyze only A diffusion.

At atmospheric pressure (this case is of practical interest), the radius of mesoscopic pores, R_p , is smaller than the mean free path of the gas molecules, and accordingly the A reactant transport occurs via the Knudsen diffusion (we neglect chromatographic effects of the walls) with the diffusion coefficient given by

$$D = \frac{2R_p}{3} \left(\frac{8k_B T}{\pi m} \right)^{1/2}, \quad (10)$$

where m is the molecule mass, and k_B the Boltzmann constant. In this regime, diffusion in a pore is essentially one-dimensional in the sense that the concentration gradients are well defined only along the pore. Specifically, the steady-state A concentration gradients in the left- and right-hand parts of the pore are $(n_A - n_A^l)/l$ and $(n_A - n_A^l)/(L - l)$, respectively. The total A diffusion flux towards the catalyst is accordingly given by

$$J_A = SD \left(\frac{n_A - n_A^l}{l} + \frac{n_A - n_A^l}{L - l} \right) \equiv \frac{SDL(n_A - n_A^l)}{l(L - l)}, \quad (11)$$

where $S = \pi R_p^2$ is the pore cross-section.

From the mass conservation law, we have

$$J_A = W_A, \quad (12)$$

where W_A is the total rate of A conversion on the catalyst particle.

If the catalyst surface is primarily covered by B (equation (8)), A desorption is negligible and accordingly the rate of A conversion equals the total rate of A adsorption,

$$W_A = (s/s_0) k_A^a n_A^l (1 - \theta), \quad (13)$$

where s is the active surface of the catalyst particle, and s_0 the area of the adsorption site. Substituting expressions (11) and (13) into equation (12) yields

$$n_A^l = n_A / [1 + \kappa(1 - \theta)], \quad (14)$$

where

$$\kappa = \frac{sk_A^a l(L - l)}{s_0 SDL}. \quad (15)$$

Substituting then expression (14) into equation (8) (with $d\theta/dt = 0$), we get

$$1 - \theta = p/[1 + \kappa(1 - \theta)], \quad (16)$$

where $p = k_A^a n_A / k_{B_2}^a n_{B_2}$. From equation (16), one can easily calculate θ and then the reaction rate as a function of p and κ for the highly reactive reaction regime.

If the catalyst surface is primarily covered by A (equation (9)), the rate of A conversion is equal to the difference of the A adsorption and desorption rates,

$$W_A = (s/s_0)[k_A^a n_A^l (1 - \theta) - k_A^d \theta]. \quad (17)$$

Substituting this expression and equation (11) into (12), one can obtain the relationship between n_A^l and n_A . Expressing then n_A^l via n_A in equation (9) (with $d\theta/dt = 0$) results in

$$(1 - \theta)^2 = \frac{(1 - \theta)p - \varphi\theta}{1 + \kappa(1 - \theta)}, \quad (18)$$

where $\varphi = k_A^d / k_{B_2}^a n_{B_2}$ (note that if the activation energy for A desorption depends on coverage, φ will also depend on coverage). Solving equation (18), one can calculate θ and then the reaction rate as a function of p and κ for the low-reactive reaction regime.

Equations (16) and (18) indicate that the diffusion limitations may be significant if κ (equation (15)) is comparable to or larger than unity. To understand the physical meaning of this condition, it is instructive to represent the A adsorption rate constant as $k_A^a = (k_B T / 2\pi m)^{1/2} s_0$, where $(k_B T / 2\pi m)^{1/2}$ is the average velocity for one of the directions (here the A sticking coefficient is assumed to be equal to unity). Substituting this expression and equation (10) into (15), we have

$$\kappa = \frac{3sl(L - l)}{8\pi L R_p^3}. \quad (19)$$

The latter expression shows that $\kappa \geq 1$ if the active area of a catalyst particle is comparable with the pore cross-section (i.e., $s \approx \pi R_p^2$) and the pore is long compared to the pore radius.

The reaction kinetics, calculated by employing the equations above, are shown in figure 2 for the case when the A diffusion limitations are negligible ($\kappa = 0$) and also for $\kappa = 1$. Two major changes are seen to occur due to the A diffusion limitations (note that there are no B₂ diffusion limitations in either case): (i) The rate maximum is shifted towards a larger A content in the reaction gas mixture (from $p = 1$ up to 2). (ii) The bistability regime is broadened. Both these effects are primarily related to the highly reactive regime. In this regime, the difference between the reaction kinetics for $\kappa = 0$ and 1 is considerable, because the A concentration gradients are significant (the local A concentration near the catalyst particle is much lower than that outside the pore). In the low-reactive regime, the reaction kinetics for $\kappa = 1$ is close to that for $\kappa = 0$, because the A diffusion can then easily maintain almost the same reactant

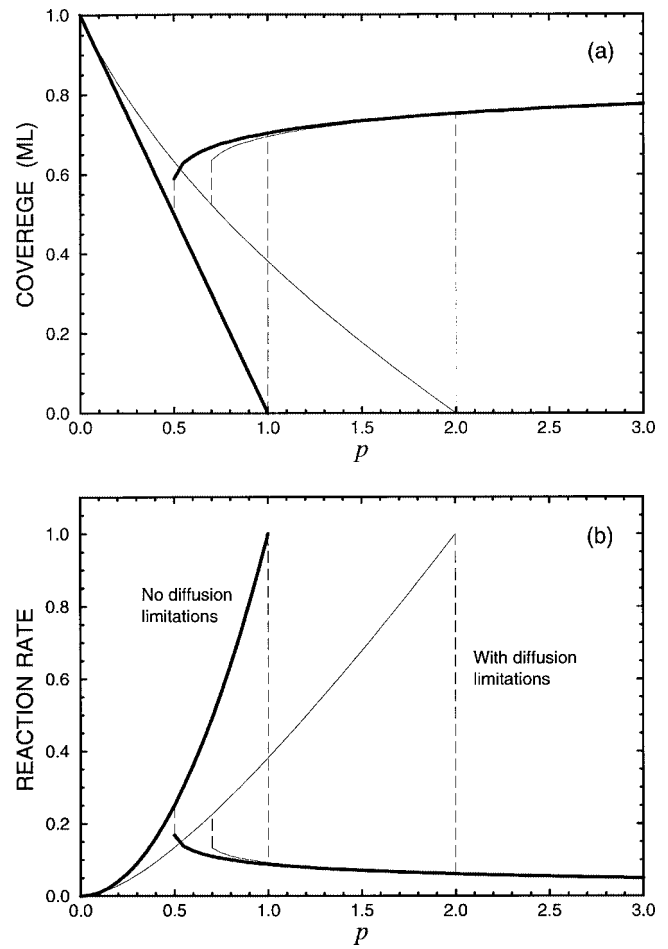


Figure 2. (a) Adsorbate coverage and (b) reaction rate (AB molecules per site per second), normalized to $k_{B_2}^a n_{B_2}$, as a function of p ($p = k_A^a n_A / k_{B_2}^a n_{B_2}$) for the cases when A diffusion limitations are negligible (thick lines) and significant (thin lines), $\kappa = 0$ and 1, respectively (there is no diffusion limitation for B₂ in either case, due to its low sticking coefficient). The dashed lines indicate step-wise changes in the reaction rate and coverage during the transitions from one reaction regime to another. During the high- and low-reactive regimes, the catalyst surface is covered by B and A, respectively. In the former case, the reaction kinetics depends only on the local reactant concentrations and the adsorption rate constants. In the latter cases, the reaction kinetics depends also on the rate of A desorption or, more specifically, on $\varphi = k_A^d / k_{B_2}^a n_{B_2}$. The A desorption rate constant used in the calculations is represented as $k_A^d = \nu_A^d \exp(-E_A^d / k_B T)$. The results were obtained for $T = 500$ K, $E_A^d = 35 - 15\theta_A$ kcal/mol, and $\nu_A^d / (k_{B_2}^a n_{B_2}) = 10^{10}$ (for $\nu_A^d = 10^{16} \text{ s}^{-1}$, this ratio corresponds to $P_{B_2} \approx 0.01$ bar).

concentrations near the catalyst, as outside the pore even if $\kappa = 1$.

From a practical point of view, it is interesting to note that diffusion limitations of A actually provide a higher absolute rate in the gas mixing regime with $1 \leq p \leq 2$. This happens because the A diffusion limitations postpone the A self-poisoning from $p = 1$ for $\kappa = 0$ to $p = 2$ for $\kappa = 1$. This result underlines the fact that kinetic phase transitions and bistability regimes in porous catalysts in general cannot be expected to occur at the same pressure values as for planar catalysts with no diffusion limitations.

In summary, our calculations indicate that the kinetics of rapid bistable reactions, running on a nm catalyst particle located in a mesoscopic pore, may be influenced by limitations on reactant diffusion via the pore space. This conclusion has important implications for using the phenomenological reaction–diffusion equations (see, e.g., equation (1)) for describing rapid reactions. In particular, the conventional assumption that the effective reaction rate constants in such equations are independent of the pore sizes may fail. This does not mean, however, that the phenomenological equations are no longer applicable, but to employ these equations, one should introduce the properly defined effective reaction rate constants taking into account diffusion limitations in single pores as was shown above.

Finally, it is appropriate to note that our results also have implications for describing oscillatory kinetics of rapid reactions occurring on nm catalysts located in mesoscopic pores. During the past decade, there have been several reports on observations of such oscillations. For example, we refer to two interesting studies of oscillatory kinetics found in CO oxidation over zeolite-supported Pd [6] and silica-supported Pt [7] under nearly isothermal conditions. In both cases, the metal crystallites with sizes about 10 nm were located primarily inside pores (even though the size of Pd particles exceeded the largest cages of the host lattice). In the former case, the total pressure and temperature were 1 atm (20 vol% O₂ and ≤0.15 vol% CO) and 450 K, respectively. In the latter case, oscillations were found at $P = 10\text{--}100$ mTorr ($0.04 \leq \text{CO/O}_2 \leq 1.7$) and $T = 400\text{--}600$ K. In analogy with single- or polycrystal samples [8], one could expect that the oscillations under consideration result from the interplay of a rapid bistable catalytic cycle and relatively slow “side” processes such as adsorbate-induced surface restructuring, oxide formation, or carbon deposition. At atmospheric pres-

sure, the most likely side process for the CO + O₂ reaction is oxide formation. In particular, the mean-field oxide model was used [9] to study synchronization of oscillations on different catalyst particles in a continuously stirred tank reactor. Monte Carlo simulations [10] based on the oxide model have shown that oscillations are possible on catalyst particles with sizes down to 5 nm. In both studies [9,10], CO diffusion limitations in single pores were neglected. Our present study shows that such limitations may actually be important in the case of long pores at least during the highly reactive reaction regime (when the oxide coverage increases).

Acknowledgement

This work was supported by the NUTEK Competence Center for Catalysis at Chalmers (grant No. 4F7-97-10929).

References

- [1] J.M. Thomas and W.J. Thomas, *Principles and Practice of Heterogeneous Catalysis* (VCH, Weinheim, 1997).
- [2] L. Zhang and N.A. Seaton, *Chem. Eng. Sci.* 49 (1994) 41.
- [3] J.S. Andrade, D.A. Street, Y. Shibusa, S. Halvin and H.E. Stanley, *Phys. Rev. E* 55 (1997) 772.
- [4] V.P. Zhdanov and B. Kasemo, *Surf. Sci. Rep.* 20 (1994) 111.
- [5] V.P. Zhdanov and B. Kasemo, *Surf. Sci. Rep.* 39 (2000) 25.
- [6] M.A. Liaw, P.J. Plath and N.J. Jaeger, *J. Chem. Phys.* 104 (1996) 6375.
- [7] J. Lauterbach, G. Bonilla and T.D. Pletcher, *Chem. Eng. Sci.* 54 (1999) 4501.
- [8] F. Schüth, B.E. Henry and L.D. Schmidt, *Adv. Catal.* 39 (1993) 51.
- [9] M.M. Slinko, E.S. Kurkina, M.A. Liaw and N.J. Jaeger, *J. Chem. Phys.* 111 (1999) 8105.
- [10] V.P. Zhdanov, *Catal. Lett.* 69 (2000) 21.